Journal of Alloys and Compounds 502 (2010) 392–395

Contents lists available at ScienceDirect

Journal of Alloys and Compounds

journal homepage: www.elsevier.com/locate/jallcom

Magnetic and inductive heating properties of Fe_3O_4/polyethylene glycol composite nanoparticles with core–shell structure

Dong-Lin Zhao[a,*], Pan Teng[b], Ying Xu[a], Qi-Sheng Xia[c], Jin-Tian Tang[d]

[a] State Key Laboratory of Chemical Resource Engineering, Beijing University of Chemical Technology, Beijing 100029, China
[b] School of Chemistry and Chemical Engineering, Sun Yat-Sen University, Guangzhou 510275, China
[c] Institute of Clinical Medical Sciences, China-Japan Friendship Hospital, Beijing 100029, China
[d] School of Medicine, Tsinghua University, Beijing 100084, China

ARTICLE INFO

Article history:
Received 2 November 2009
Received in revised form 18 April 2010
Accepted 25 April 2010
Available online 4 May 2010

Keywords:
Nanostructures
Nanofabrications
Scanning and transmission electron microscopy
X-ray diffraction
Magnetic measurements

ABSTRACT

The magnetite (Fe_3O_4) nanoparticles were prepared by coprecipitation of Fe^{3+} and Fe^{2+} using ammonium hydroxide (NH_4OH) as a precipitating agent. The Fe_3O_4/polyethylene glycol (PEG) magnetic composite nanoparticles with a core–shell structure with a diameter of 10–40 nm were prepared by two step additions of the primary and the secondary surfactants, respectively. The inductive heat property of Fe_3O_4/PEG composite nanoparticles in an alternating current (AC) magnetic field was investigated. The potential of Fe_3O_4/PEG nanoparticles was evaluated for localized hyperthermia treatment of cancers. The saturation magnetization, *Ms*, and coercivity, *Hc*, are 67.06 emu g^{-1} and 7 Oe for Fe_3O_4 nanoparticles and 64.11 emu g^{-1} and 14 Oe for Fe_3O_4/PEG composite nanoparticles, respectively. Exposed in the AC magnetic field for 100 s, the temperatures of physiological saline suspensions containing Fe_3O_4 nanoparticles or Fe_3O_4/PEG composite nanoparticles are 89.2 °C and 72.2 °C, respectively. The Fe_3O_4/PEG composite nanoparticles will be useful as good thermoseeds for localized hyperthermia treatment of cancers.

1. Introduction

Hyperthermia is a promising approach to cancer therapy [1,2]. The inevitable technical problem with hyperthermia is the difficulty in heating only the local tumor region to the intended temperature without damaging the surrounding healthy tissue. Fe_3O_4 nanoparticles have been used for hyperthermia treatment in an attempt to overcome this obstacle [3,4]. If Fe_3O_4 nanoparticles can be made to accumulate only in the tumor tissue, cancer-specific hyperthermia can be achieved by generating heat in an alternating current (AC) magnetic field due to hysteresis loss [5]. Localized hyperthermia treatment of cancers injects the magnetic thermoseeds into the tumor area of the patient. The heating of the cancer area containing the implanted thermoseeds to elevated temperatures in an external AC magnetic field induces apoptosis of tumor cells. Due to the strong magnetic property and low toxicity, the application of Fe_3O_4 in biotechnology and medicine has attracted significant attention [6–16]. Magnetic fluid hyperthermia (MFH) is an important application, which can increase the temperature of tumors to 41–46 °C and therefore kill tumor cells. This method involves the introduction of ferromagnetic or superparamagnetic particles (thermoseeds) into the tumor tissue and then irradiation with an AC magnetic field. The particles transform the energy of the AC magnetic field into heat by several physical mechanisms, and the transformation efficiency strongly depends on the frequency of the external field as well as the nature of the particles such as magnetism and surface modification [17–22].

With the rapid development of nanotechnology, it has become possible to fabricate, characterize and specially tailor the functional properties of nanoparticles for biomedical applications and diagnostics [22–26]. Increased investigations with several types of iron oxides have been carried out in the field of nanosized magnetic particles, among which Fe_3O_4 is a very promising candidate since its biocompatibility has already been proven [22]. With proper surface coatings, these magnetic nanoparticles can be dispersed into suitable solvents, forming homogeneous suspensions, called ferrofluids [27]. Such a suspension can interact with an external magnetic field and be positioned to a specific area, facilitating magnetic resonance imaging for medical diagnosis and AC magnetic field-assisted cancer therapy [22]. Fe_3O_4 has been widely studied in recent years due to its interesting magnetic properties and many potential applications, especially being an ideal candidate for biological applications [28–42].

In our previous work, Fe_3O_4 nanoparticles with different magnetic properties were prepared by coprecipitation of Fe^{3+} and Fe^{2+} and their inductive heating properties were investigated [43]. In this work, Fe_3O_4/polyethylene glycol (PEG) magnetic composite nanoparticles with a core–shell structure were prepared and their

* Corresponding author. Tel.: +86 10 64434914; fax: +86 10 64454912.
E-mail address: dlzhao@mail.buct.edu.cn (D.-L. Zhao).

0925-8388/$ – see front matter © 2010 Elsevier B.V. All rights reserved.
doi:10.1016/j.jallcom.2010.04.177

inductive heating property was measured by an AC magnetic field generator for localized hyperthermia.

2. Experimental

2.1. Preparation of Fe_3O_4 nanoparticles

$FeCl_2{\cdot}4H_2O$ and $FeCl_3{\cdot}6H_2O$ were used as iron sources and ammonium hydroxide (NH_4OH) was used as a precipitator. The iron solution was strongly stirred with 100 ml of distilled water, which was heated up to 80 °C. The molar ratio of Fe^{2+} and Fe^{3+} was 5.5:1. After stirring for 10 min, ammonium hydroxide was added. This coprecipitation process is as follows:

$$FeCl_2 + 2FeCl_3 + 8NH_4OH \rightarrow Fe_3O_4 + 8NH_4Cl + 4H_2O$$

The precipitates were separated by magnetic decantation with ethanol and distilled water after cooling of the suspension at room temperature. The subsided Fe_3O_4 nanoparticles were dried in a vacuum atmosphere at 60 °C.

2.2. Synthesis of Fe_3O_4/PEG composite nanoparticles

Fe_3O_4/PEG magnetic composite nanoparticles with a core–shell structure were prepared by two step additions of the primary and the secondary surfactants, respectively. The whole procedure was as follows. Deionized water of 60 ml was added to Fe_3O_4 nanoparticles (1.0 g) in a 250 ml round-bottomed four-necked flask equipped with a mechanical stirrer, an inlet of nitrogen and a condenser. To reduce aggregation of Fe_3O_4 nanoparticles, the mixture was kept under ultrasonic vibration for 30 min. The mixture of water and Fe_3O_4 nanoparticles was vigorously stirred for 30 min under nitrogen protection, which was heated up to 80 °C, and then a solution of 25 ml oleate sodium was added to the mixture with slow agitation. The surface modification procedure was allowed to proceed for additional 30 min. The suspension was then cooled slowly down to 50 °C with constant stirring. The PEG-4000 solution was then added to the suspension. Then, the mixture was kept at 50 °C under vigorous stirring and nitrogen protection for 1 h. The products were dialyzed and purified by magnetic field separation and decantation with water after cooling of the suspension at room temperature. This purification procedure was repeated five times. The products were dried under vacuum at 60 °C for 10 h.

2.3. Characterization of Fe_3O_4/PEG composite nanoparticles

Particle size and morphology of Fe_3O_4 and Fe_3O_4/PEG nanoparticles were detected using a Hitachi H-800 transmission electron microscope (TEM). Samples for TEM measurement were prepared by dispersing the Fe_3O_4 or Fe_3O_4/PEG nanoparticles in acetone at an appropriate concentration and then depositing on Formvar-coated copper grids and drying. The microstructure of the Fe_3O_4 and Fe_3O_4/PEG nanoparticles was characterized by powder X-ray diffraction (XRD), which was carried out in a Rigaku D/MAX-3CX diffractometer using the Kα line of Cu as a radiation source. The infrared (IR) spectra of all samples were recorded on a Nicolet 200SXV Fourier transform infrared spectrometer (FTIR) using KBr pellets. Their magnetic properties were measured by a vibration sample magnetometer (VSM, Lakeshore, Model 7300).

The inductive heating property of the Fe_3O_4/PEG composite nanoparticles was measured by an AC magnetic field generator in agreement with the method reported in Ref. [43]. Depending on body cross-section and tissue conductivity, lower frequencies in the range of 50–100 kHz should be used with humans [18]. The frequency applied in the present work is 80 kHz, which is just in the range for biomedical applications. All samples used in the measurements were freshly prepared. The frequency and amplitude of the magnetic field are 80 kHz and 30 kA m^{-1}, respectively. All samples were dispersed in physiological saline with the same concentration of 30 mg ml^{-1} and treated with ultrasound for 30 min before the measurements.

3. Results and discussion

The Fe_3O_4/PEG magnetic composite nanoparticles with a core–shell structure were prepared by two step additions of the primary and the secondary surfactants, respectively. Fig. 1(a) shows the TEM micrograph of Fe_3O_4 nanoparticles. The particles are almost spherical with diameters ranging from 5 nm to 30 nm. Most of the particles are polydisperse while some agglomerated due to magneto-dipole interactions between particles. In the absence of any surface coating, Fe_3O_4 nanoparticles have hydrophobic surfaces with a large surface area to volume ratio. Due to hydrophobic interactions between the particles, these particles agglomerate and form large clusters, resulting in increased particle size. These clusters, then, exhibit strong magnetic dipole–dipole attractions between them and show ferromagnetic behaviour. When two large-particle clusters approach one another, each of them comes into the magnetic field of the neighbour. Besides the arousal of attractive forces between the nanoparticles, each nanoparticle is in the magnetic field of the neighbour and gets further magnetized. The adherence of remnant magnetic nanoparticles causes a mutual magnetization, resulting in increased aggregation properties [22]. Fig. 1(b) shows the TEM micrograph of Fe_3O_4/PEG composite nanoparticles with a core–shell structure, which are quite polydispersed with a diameters ranging from 10 nm to 40 nm. The non-covalent immobilization of PEG on the surface can improve the biocompatibility, blood circulation time and internalization efficiency of the Fe_3O_4 nanoparticles. With PEG surface coating, the Fe_3O_4 nanoparticles were dispersed into suitable solvents, forming homogeneous suspensions, called ferrofluid. The Fe_3O_4 ferrofluid can interact with an external magnetic field and be positioned to a specific area, facilitating AC magnetic field-assisted cancer therapy. But the samples for TEM measurement were prepared by dispersing the Fe_3O_4/PEG nanoparticles in acetone at an appropriate concentration and then depositing them on the Formvar-coated copper grids and drying. So the Fe_3O_4/PEG composite nanoparticles agglomerated again due to magneto-dipole interactions between particles.

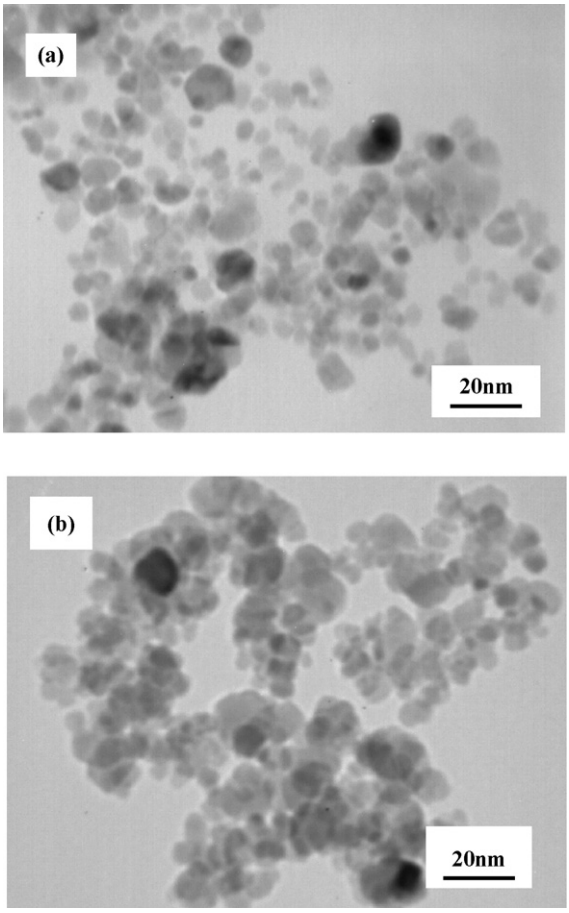

Fig. 1. TEM images of Fe_3O_4 (a) and Fe_3O_4/PEG composite nanoparticles (b).

Fig. 2 shows the XRD patterns of the Fe_3O_4/PEG composite nanoparticles as well as the Fe_3O_4 nanoparticles. XRD and electronic diffraction (ED) of Fe_3O_4 and Fe_3O_4/PEG nanoparticles indicated the inverse cubic spinel structure of Fe_3O_4. The main peaks of Fe_3O_4 and Fe_3O_4/PEG nanoparticles are at $2\theta = 18.29°$, 30.09°, 35.43°, 37.07°, 43.07°, 53.44°, 56.96°, 62.55°, 70.96°, 74.01°, 78.97°, 86.75° and 89.65°, which are observed in the pure Fe_3O_4 particles' graph. This result also indicated that the Fe_3O_4/PEG composite nanoparticles contain Fe_3O_4. The FTIR spectra of the

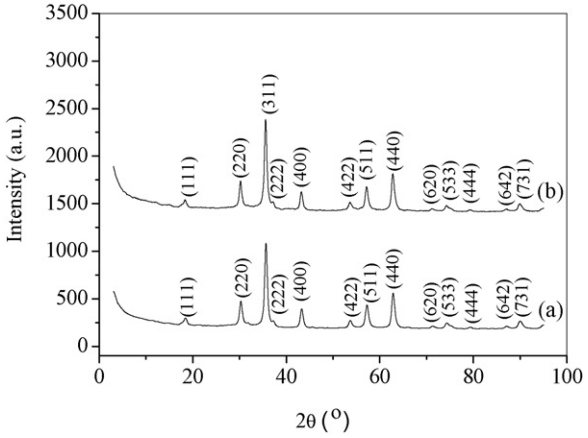

Fig. 2. XRD patterns of Fe_3O_4/PEG composite nanoparticles (a) and Fe_3O_4 nanoparticles (b).

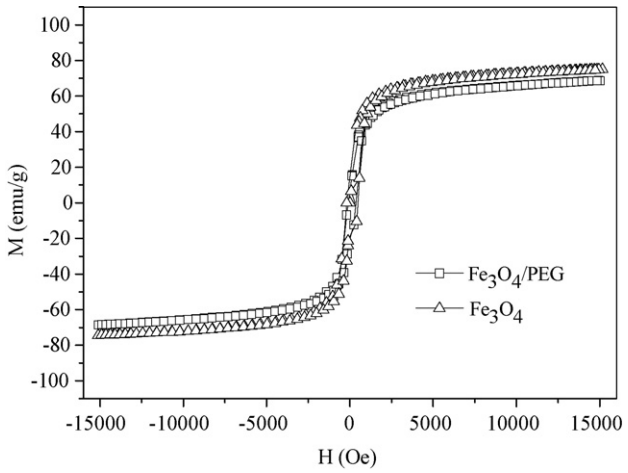

Fig. 4. Hysteresis loops of Fe_3O_4 nanoparticles and Fe_3O_4/PEG composite nanoparticles.

Fe_3O_4/PEG composite nanoparticles as well as PEG and Fe_3O_4 nanoparticles are shown in Fig. 3. The peak around 3440 cm^{-1} ascribes to the–OH group. For the Fe_3O_4/PEG and Fe_3O_4 nanoparticles, the peaks at 569 cm^{-1} ascribe to Fe–O group (Fig. 3(b) and (c)). Two typical bands near 1457.94 cm^{-1} and 1616.08 cm^{-1} indicated a complex reaction between hydroxy groups on the surface of Fe_3O_4 nanoparticles and carboxylate groups of oleate sodium [44]. The absorption of free oleate sodium, which is around 1700–1750 cm^{-1} (C=O) cannot be found. The –C=C– group of oleate sodium was characterized by band at 952.67 cm^{-1}. Absorptions at 1114.55 cm^{-1} (–C–O–C–) and 3409.58 cm^{-1} (the associated hydroxy groups) indicated the existence of PEG. This result suggested that the Fe_3O_4 nanoparticles be successfully coated by oleate sodium and PEG-4000.

Saturation magnetization *Ms*, remanent magnetization *Mr* and coercivity *Hc* are the main technical parameters to characterize the magnetism of a ferromagnetic particle sample. The hysteresis loops of Fe_3O_4 nanoparticles and Fe_3O_4/PEG composite nanoparticles are shown in Fig. 4. *Ms* and *Hc* are 67.06 emu g^{-1} and 7 Oe for Fe_3O_4 nanoparticles and 64.11 emu g^{-1} and 14 Oe for Fe_3O_4/PEG composite nanoparticles, respectively.

It can be seen that Ms, *Mr*, *Hc*, and *Mr*/*Ms* of Fe_3O_4 nanoparticles are higher than those of Fe_3O_4/PEG composite nanoparticles. Fig. 5 shows the time-dependent temperature curves of Fe_3O_4 nanoparticles and Fe_3O_4/PEG composite nanoparticles in the 80 kHz and 30 kA m^{-1} AC magnetic field. As shown in Fig. 5, exposed in the 80 kHz and 30 kA m^{-1} AC magnetic field for 100 s, the temperatures of physiological saline suspensions containing Fe_3O_4 nanoparticles or Fe_3O_4/PEG composite nanoparticles with a concentration of 30 mg ml^{-1} are 89.2 °C and 72.2 °C, respectively. The heating of the cancer area containing the implanted thermoseeds to elevated temperatures of 41–46 °C in an external AC magnetic field kills tumor cells. So the Fe_3O_4/PEG composite nanoparticles with a core–shell structure can be used as thermoseeds for localized hyperthermia treatment of cancers.

The inductive heating of oxide magnetic materials with low electrical conductivity in an external AC magnetic field is due to the loss processes during the reorientation of the magnetization. If thermal energy k_BT is too low to facilitate reorientation, hysteresis losses dominate which depend on the type of remagnetization process (wall displacement or several types of rotational processes). With decreasing particle size thermal activation of reorientation processes lead in dependence on temperature and measurement frequency to superparamagnetic behaviour of the particle ensemble and the occurrence of the so-called Néel relaxations losses. In the case of ferrofluids losses related to the rotational Brownian motion of magnetic particles may arise, too [45]. Relaxation losses are caused by the relaxation processes of ultrafine monodomain magnetic particles in an AC magnetic field, which are the gradual

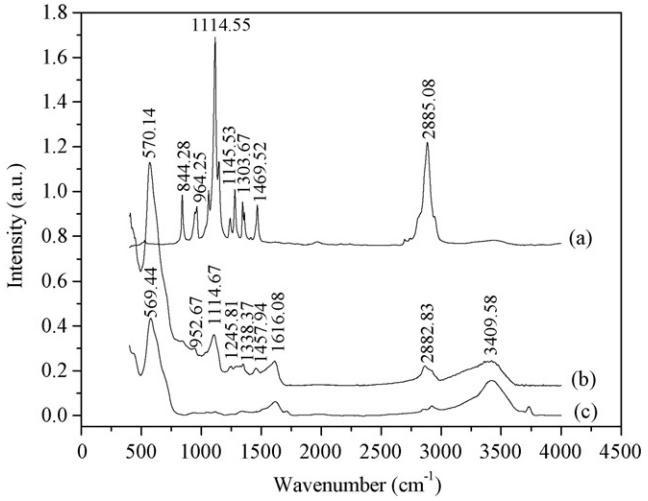

Fig. 3. FTIR spectra of PEG (a), Fe_3O_4/PEG composite nanoparticles (b) and Fe_3O_4 nanoparticles (c).

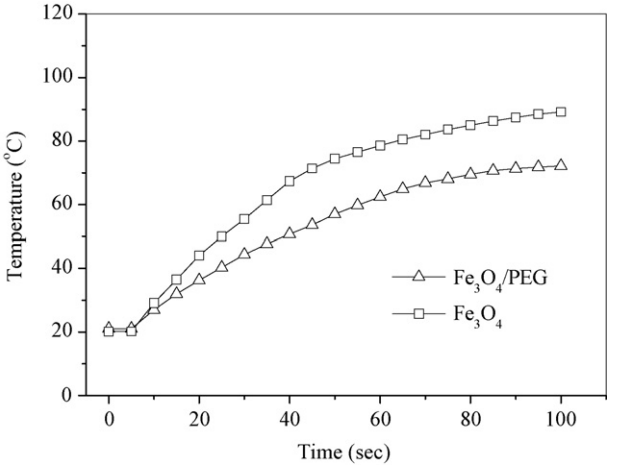

Fig. 5. Time-dependent temperature curves of Fe_3O_4/PEG composite nanoparticles and Fe_3O_4 nanoparticles in the 80 kHz and 30 kA m^{-1} AC magnetic field.

alignment of the magnetic moments during the magnetization process. The relaxation processes of a ferrofluid may take place through two distinct mechanisms. The first one consists of the rotation of the single-domain particle, which is related to the Brownian motion of the magnetic particles. The second one corresponds to magnetization vector rotation if we abstract the Brownian motion and consider the particle immobile. The second one is the so-called Néel relaxation of fine magnetic particles. Ferrofluid can exhibit both of these mechanisms, each having the proper weight [17]. Both Néel and Brownian relaxations contribute to the power losses of the Fe_3O_4 and Fe_3O_4/PEG nanoparticles. Hysteresis loss is mainly due to the domain wall motion, and its value is given by the area of the hystersis loop in an applied AC magnetic field [17]. For the magnetic materials whose saturation magnetization *Ms* is high, their specific power absorption will be big. So the inductive heating property of Fe_3O_4 nanoparticles in the AC magnetic field is higher than that of Fe_3O_4/PEG composite nanoparticles (Fig. 5).

4. Conclusions

The Fe_3O_4 nanoparticles were prepared by coprecipitation of Fe^{3+} and Fe^{2+} using ammonium hydroxide as a precipitating agent. The Fe_3O_4/PEG magnetic composite nanoparticles with a core–shell structure with a diameter of 10–40 nm were prepared by two step additions of the primary and the secondary surfactants, respectively. The saturation magnetization, *Ms*, and coercivity, *Hc*, are 67.06 emu g^{-1} and 7 Oe for Fe_3O_4 nanoparticles and 64.11 emu g^{-1} and 14 Oe for Fe_3O_4/PEG composite nanoparticles, respectively. Exposed in the AC magnetic field for 100 s, the temperatures of physiological saline suspensions containing Fe_3O_4 nanoparticles or Fe_3O_4/PEG composite nanoparticles are 89.2 °C and 72.2 °C, respectively. The Fe_3O_4/PEG composite nanoparticles can be used as thermoseeds for localized hyperthermia treatment of cancers.

Acknowledgements

This work was supported by the National Natural Science Foundation of China (Grant No. 50672004) and the National High-Tech Research and Development Program (2008AA03Z513).

References

[1] J. van der Zee, Annu. Oncol. 13 (2002) 1173–1184.
[2] P. Moroz, S.K. Jones, B.N. Gray, Int. J. Hyperther. 18 (2002) 267–284.
[3] A. Jordan, P. Wust, H. Fahling, Int. J. Hyperther. 9 (1993) 51–68.
[4] T. Minamimura, H. Sato, S. Kasaoka, Int. J. Oncol. 16 (2000) 1153–1158.
[5] A. Ito, Y. Kuga, H. Honda, H. Kikkawa, A. Horiuchi, Y. Watanabe, T. Kobayashi, Cancer Lett. 212 (2004) 167–175.
[6] P. Yang, Z. Quan, Z. Hou, C. Li, X. Kang, Z. Cheng, J. Lin, Biomaterials 30 (2009) 4786–4795.
[7] W. Zhou, W. He, S. Zhong, Y. Wang, H. Zhao, Z. Li, S. Yan, J. Magn. Magn. Mater. 321 (2009) 1025–1028.
[8] F.J. Xu, K.G. Neoh, E.T. Kang, Prog. Polym. Sci. 34 (2009) 719–761.
[9] H. Sun, X. Zhu, L. Zhang, Y. Zhang, D. Wang, Mater. Sci. Eng. C 30 (2010)311–315.
[10] H. Basti, L.B. Tahar, L.S. Smiri, F. Herbst, M.J. Vaulay, F. Chau, S. Ammar, S. Benderbous, J. Colloid Interface Sci. 341 (2010) 248–254.
[11] R. Zhang, C. Wu, X. Wang, Q. Sun, B. Chen, X. Li, S. Gutmann, G. Lv, Mater. Sci. Eng. C 29 (2009) 1697–1701.
[12] P. Pouponneau, J.C. Leroux, S. Martel, Biomaterials 30 (2009) 6327–6332.
[13] S. Guo, D. Li, L. Zhang, J. Li, E. Wang, Biomaterials 30 (2009) 1881–1889.
[14] J. Xie, K. Chen, J. Huang, S. Lee, J. Wang, J. Gao, X. Li, X. Chen, Biomaterials 31 (2010) 3016–3030.
[15] A. Zhu, L. Yuan, W. Jin, S. Dai, Q. Wang, Z. Xue, A. Qin, Acta Biomater. 5 (2009) 1489–1498.
[16] F. Yang, Y. Li, Z. Chen, Y. Zhang, J. Wu, N. Gu, Biomaterials 30 (2009) 3882–3890.
[17] M. Ma, Y. Wu, J. Zhou, Y. Sun, Y. Zhang, N. Gu, J. Magn. Magn. Mater. 268 (2004) 33–39.
[18] A. Jordan, R. Scholz, P. Wust, H. Fähling, R. Felix, J. Magn. Magn. Mater. 201 (1999) 413–419.
[19] O.S. Nielsen, M. Horsman, J. Overgaard, Eur. J. Cancer 37 (2001) 1587–1589.
[20] A. Jordan, R. Scholz, P. Wust, H. Schirra, J. Magn. Magn. Mater. 194 (1999) 185–196.
[21] R. Hergta, R. Hiergeista, M. Zeisberger, G. Glöckl, W. Weitschies, L.P. Ramirez, I. Hilger, W.A. Kaiser, J. Magn. Magn. Mater. 280 (2004) 358–368.
[22] A.K. Gupta, M. Gupta, Biomaterials 26 (2005) 3995–4021.
[23] S.M. Moghimi, A.C.H. Hunter, J.C. Murray, Pharm. Rev. 53 (2001) 283–318.
[24] A.S.G. Curtis, C. Wilkinson, Trends Biotechnol. 19 (2001) 97–101.
[25] J.M. Wilkinson, Med. Device Technol. 14 (2003) 29–31.
[26] J. Panyam, V. Labhasetwar, Adv. Drug Deliv. Rev. 55 (2003) 329–347.
[27] Y.X. Wang, S.M. Hussain, G.P. Krestin, Eur. Radiol. 11 (2001) 2319–2331.
[28] A. Yan, X. Liu, G. Qiu, H. Wu, R. Yi, N. Zhang, J. Xua, J. Chen, J. Alloys Compd. 458 (2008) 487–491.
[29] A.P.A. Faiyas, E.M. Vinod, J. Joseph, R. Ganesan, R.K. Pandey, J. Magn. Magn. Mater. 322 (2010) 400–404.
[30] X.H. Liu, W.B. Cui, W. Liu, X.G. Zhao, D. Li, Z.D. Zhang, J. Alloys Compd. 475 (2009) 42–45.
[31] L. Gu, H. Shen, J. Alloys Compd. 472 (2009) 50–54.
[32] W. Lu, Y. Shen, A. Xie, W. Zhang, J. Magn. Magn. Mater. 322 (2010) 1828–1833.
[33] R. Valenzuela, M.C. Fuentes, C. Parra, J. Baeza, N. Duran, S.K. Sharma, M. Knobel, J. Freer, J. Alloys Compd. 488 (2009) 227–231.
[34] H. Yan, J. Zhang, C. You, Z. Song, B. Yu, Y. Shen, Mater. Chem. Phys. 113 (2009) 46–52.
[35] R. Shi, X. Liu, G. Gao, R. Yi, G. Qiu, J. Alloys Compd. 485 (2009) 548–553.
[36] R.Y. Hong, B. Feng, G. Liu, S. Wang, H.Z. Li, J.M. Ding, Y. Zheng, D.G. Wei, J. Alloys Compd. 476 (2009) 612–618.
[37] D.L. Zhao, X.X. Wang, Q.S. Xia, J.T. Tang, J. Alloys Compd. 477 (2009) 739–743.
[38] J. Chen, F. Wang, K. Huang, Y. Liu, S. Liu, J. Alloys Compd. 475 (2009) 898–902.
[39] L. Li, Y. Chu, Y. Liu, D. Wang, J. Alloys Compd. 472 (2009) 271–275.
[40] T. Ozkaya, M.S. Toprak, A. Baykal, H. Kavas, Y. Koseoglu, B. Aktas, J. Alloys Compd. 472 (2009) 18–23.
[41] H. Hu, Z. Wang, L. Pan, J. Alloys Compd. 492 (2010) 656–661.
[42] X. Zhang, Q. Dai, X. Huang, X. Tang, Solid State Sci. 11 (2009) 1861–1865.
[43] D.L. Zhao, X.W. Zeng, Q.S. Xia, J.T. Tang, J. Alloys Compd. 469 (2009) 215–218.
[44] R.Y. Hong, S.Z. Zhang, Y.P. Han, H.Z. Li, J. Ding, Y. Zheng, Powder Technol. 170 (2006) 1–11.
[45] R. Hiergeist, W. Andrä, N. Buske, R. Hergt, I. Hilger, U. Richter, W. Kaiser, J. Magn. Magn. Mater. 201 (1999) 420–422.